Direct ink write multi-material printing of PDMS-BTO composites with MWCNT electrodes for flexible force sensors

Anabel Renteria[1,2,3], Victor H. Balcorta[1,2,3], Aaron A. Rodriguez[1,2], Cory Marquez[1,2,3], Ivan Renteria-Marquez[3], Jaime Regis[1,2], Bethany Wilburn[4], Steven Patterson[4], David Espalin[1,2], Tzu-Liang (Bill) Tseng[3], Yirong Lin[1,2]

[1]*Department of Mechanical Engineering, The University of Texas at El Paso, El Paso, 79968, United States.*
[2]*W.M. Keck Center for 3D Innovation, The University of Texas at El Paso, El Paso, 79968, United States.*
[3]*Department of Industrial, Manufacturing, and Systems Engineering, The University of Texas at El Paso, El Paso 79968, United States.*
[4]*Kansas City National Security Campus, Kansas City 64147, United States.*

**Corresponding author E-mail:* arenteriamarquez@miners.utep.edu

Keywords: Multi-material printing, piezoelectric devices, flexible force sensors

Abstract

With recent advances of technology of additive manufacturing (AM), direct ink write (DIW) printing has allowed to incorporate multi-material printing of various materials with freedom of design and complex geometric printing to complete functional sensors in a one-step fabrication. This paper introduces the fabrication of polydimethylsiloxane (PDMS) with barium titanate (BTO) as a high stretchable composite with increased piezoelectric properties that can be used for force sensors applications. To help improve the bonding of the materials and improvement in the piezoelectric coefficient, multi-wall carbon nanotubes (MWCNT) was included in the fabrication of electrodes at a fixed ratio of 11 wt. %. The alignment of the BTO dipoles was through corona poling method, which applies an electric charge on the layer surface of the functional material, aligning the dipoles in the desired direction and improving the piezoelectricity. Different BTO mixing ratios (10-50 wt. %) were evaluated in order to obtain tunable piezoelectric properties and compare the sensitivity with respect their elastic properties. Further testing included tensile and compression loading testing to determined Young's modulus and voltage output showing the flexibility and sensibility of the force sensor. Results showed that fabricated PDMS with 50 wt. % BTO gave the highest piezoelectric coefficient (d_{33}) of 11.5 pC/N and with an output voltage of 385 mV under compression loading of >200 lbF. This demonstrates feasibility of using multi-material DIW printing to fabricate one-step force sensors with high piezoelectric coefficients without compromising the flexibility of the material.

1. Introduction

Piezoelectric ceramics have been of great interest in the past years due to the large number of applications that can be used for sensing, actuating and energy harvesting. Among all piezoelectric ceramics, barium titanate (BTO) is one of the most used lead-free ceramics due to its good piezoelectric (d33: ~ 191 pC/N) [1] and dielectric (ε ~1700 at room temperature) [2] properties compared to lead piezoelectric ceramics such as lead zirconate titanate (PZT). Although piezoelectric ceramics have been widely used for industrial applications, such as aerospace and healthcare, there is still limited range of functionality since ceramics are brittle by nature and non-conformable. With the increased demand on flexible wearable devices, such as force sensors that must directly interact with the human body to monitor dynamic pressure signals has led to an increased research interest to develop lead-free devices [3].

Polydimethylsiloxane (PDMS) is one the most reported thermoset silicone elastomers due to its biocompatibility and low Young's elastic modulus E ~ 1-3 MPa, [4] providing great flexibility and compliance to adapt to different surfaces. Previous efforts on fabrication of force sensors with high flexibility fabricated by traditional casting reported the use of piezoelectric ceramic particles as a functional filler, mainly including the use of BTO and PZT [5], [6]. However, the samples manufactured through casting has been restricted to films, in which it has been difficult to control final thickness and density of the films. In addition, PDMS is characterized to have low surface tension and hydrophobic properties, which makes it difficult to electrode [4]. For that reason, PDMS usually requires a surface treatment with plasma allowing it temporary hydrophilic properties to be able to apply electrodes or coatings [4]. Nonetheless, surface treatments typically provide a poor material bonding between PDMS and the electrodes, affecting the elasticity and mechanical properties. An alternative to surface treatments is the development of polymer composites with highly conductive materials fillers, including carbon allotropes, silver and gold nanoparticles [7]. The percolation threshold at a lower molecular weight plays a significant role to select the conductive material while avoiding compromising the device's flexibility. Multi-wall carbon nanotubes (MWCNT) is a semiconductor material known to have good electrical properties that reach percolation threshold at low weight percentages. This is possible due to MWCNT's high aspect ratio of tubular structures that produces a more effective electron conductive network [7]. In addition, MWCNT has good piezoresistive properties making it ideal for the development of strain and force sensors.

Direct ink write (DIW) is a material extrusion 3D printing technique that selectively deposits an ink through a nozzle to form a three-dimensional part. DIW is an easy technique used for rapid prototyping, in which by controlling rheological properties it is possible to adapt for a large material selection and wide molecular weights. One of the requirements for DIW is to obtain shear thinning behavior and a solid-like behavior under low shear rates to guarantee self-support after deposition during printing, which can be easily adaptable to printing composites [8]. However, one of the main drawbacks of DIW is the low resolution of the 3D printed parts due to the nature of the ink, which can be improved by controlling the rheological properties. Another drawback of using DIW technique is that the samples require a post-treatment process to solidify, including thermal curing or photopolymerization. This post-treatment has to be designed according to the type of material (i.e., ceramics, elastomers) to prevent the formation of quality defects such as voids, cracks or warping of the samples. Despite that, the biggest advantage of using DIW technique is that the fabricated parts usually resulted on high-density samples with tunable mechanical properties [9], [10]. In addition, DIW multi-material extrusion is possible by having multiple printing heads, which has enabled the fabrication of structures with multiple materials at the same time. Multi-material extrusion has been reported in the past to fabricated elaborate designs by DIW technique, using the additional material as sacrificial support structure in the fabrication of composites and ceramics [10], [11]. However, there is very limited work on the development of DIW multi-material extrusion to fabricate piezoelectric ceramics or composites. It is expected to see a huge impact in the development of electronic devices, reducing waste and fabrication time while improving material bonding and mechanical properties.

This work presents a novel fabrication method using DIW multi-material extrusion 3D printing technique for PDMS-BTO composites for force sensors applications. To overstand the limitation of having to apply a surface treatment to change the hydrophobicity of PDMS, a slurry with MWCNT was developed improving the material bonding compared to using coatings. The effect of BTO content in the PDMS matrix was evaluated to see the impact on the piezoelectric properties, young's elastic modulus, and output voltage, which define the functionality of force sensors to capture pressure signals. The results obtained in the force

sensors proves the feasibility of using DIW multi-material printing technique to fabricate complete sensors in a single step.

2. Experimental section

Materials: For the piezoelectric composite two different types of polydimethylsiloxane (PDMS) were used as the thermoset matrix (Dowsil 1700; viscosity ~ 542 Pa-sec and Dow Sygard 184; viscosity ~ 5.1 Pa-sec) to control rheological properties and assure printability. Barium Titanate (BTO) powder (Goodfellow; maximum particle size 45 μm) was used as the functional piezoelectric filler. For the conductive ink PDMS (Dow Sygard 184) was used as a matrix and Multi-Wall Carbon Nanotubes (MWCNT) (Cheaptubes; diameter: 8-15 nm, length: 10-50 micron) were used as conductive fillers.

PDMS-BTO ink fabrication: The PDMS ink preparation consisted of PDMS (Dowsil 1700) and PDMS (Dow Sygard 184) used at a 8:2 ratio. Each PDMS was prepared using a standard mixing ratio between the base and catalyst of 10:1. The BTO content varied from 10 wt. % to 50 wt. % with respect of the PDMS matrix. The ink was mixed using a planetary centrifugal mixer (Thinky; Laguna Hills, CA) at 2000 rpm was used for mixing and 2200 rpm for defoaming for 30 seconds each cycle. The mixing cycle helped to avoid agglomeration of particles in the ink during printing. The ink was deposited inside EMO-25 metal containers so it can be used for DIW printing.

MWCNT electrodes fabrication: To fabricate the conductive electrodes' ink, the PDMS (Dow Sygard 184) matrix was used in a 10:1 ratio for the base to catalyst and was mixed with 11 wt. % MWCNT. The PDMS-MWCNT ink was mixed with the planetary centrifugal mixer using the same parameters used for the BTO-PDMS ink preparation. After mixing, the PDMS-MWCNT ink was loaded in an EMO-25 metal container for future DIW printing.

The samples were fabricated using a Hyrel 30M printer (Hyrel 3D; Norcross, GA) with dual high-viscous extruders (EMO-25; $\eta \sim 300$ Pa.s) for slurry deposition at room temperature. The g-codes of the STL models were created thorough Slic3r software while the printing process was performed using Repetrel software. Different geometries were fabricated by DIW multi-material extrusion, rectangular samples with dimensions of 15 x 10 x 1.60 mm for piezoelectric and dielectric measurements. Compression disks of 40 mm diameter and 3 mm thickness for output voltage measurements. Dogbones structures for tensile testing according to the standard for elastomers (ASTM 412D). Samples were printed using a nozzle diameter of 500 μm for both materials, the electrodes thickness was set to 300 μm for all the samples. After printing, the samples were cured in a Form Cure (Formlabs; Somerville, MA) at 70 °C for 90 minutes.

Material characterization

Rotational rheological measurements for the composite inks were performed in a DHR-2 rheometer (TA Instruments, New Castle, DE) with a parallel plate geometry. The test was performed at 24 °C with a 0.7 mm gap between the plates. Bonding between electrodes and PDMS-BTO composites and BTO powder dispersion was characterized from the cross-sectional surface by using scanning electron microscopy (SEM; JEOL, JSM-IT500HR) under low vacuum, 20.0 kV accelerating voltage using backscatter electron. The piezoelectric coefficient was calculated using a d_{33} meter (APC YE2730A) by applying a load of 0.25 N at a frequency of 110 Hz. The dielectric constant of the samples was determined by measuring the capacitance using an LCR meter (1920 Precision, IET Lab) at room temperature (24 °C) at a frequency of 1 kHz. Tensile and cyclic compression testing were performed using a motorized test stand ESM1500 (Mark-10, Copiague, NY). Voltage output during cyclic compression loading was registered with an oscilloscope (Rigol DS1102E, Beaverton, OR).

3. Results and discussions

3.1 Rheological measurements

The inks were designed considering the rheological properties needed for DIW multi-material extrusion aiming for good printability and self-support after deposition. The printability and viscosity of the inks was highly influenced by two different factors, the ratio of the two different PDMS silicone (Dowsil 1700 and Dow Sygard 184) and the weight percentage of functional filler dispersed in the matrix. Rheological measurements were performed for different inks varying the BTO content from 10 to 50 wt. % to evaluate their impact on their viscoelastic properties. The PDMS-BTO inks showed a shear thinning behavior, in which the viscosity was reduced when increasing the applied shear rates as shown in Figure 1 (a). This behavior on the material flow was partially attributed to the PDMS (Dowsil 1700 and Dow Sygard 184) mixture ratio, that increased the complex viscosity of the ink and the energy required to distort it also known as storage modulus (*G'*), which contributed to guarantee self-support. In addition, the BTO powder contributed to the shear thinning behavior of the inks due to an evident increase in the viscosity for the inks with higher BTO content, which was produced due to a restriction on the particles mobility in the matrix [12]. The viscoelastic properties of the inks as shown in Figure 1 (b) were measured at 24 °C and 5% strain varying angular velocity. It was found a dominant elastic behavior for the inks (*G' > G"*) at different angular frequencies, which indexed for solid-like inks that could be adaptable to 3D printing and self-support after deposition under low shear rates [13].

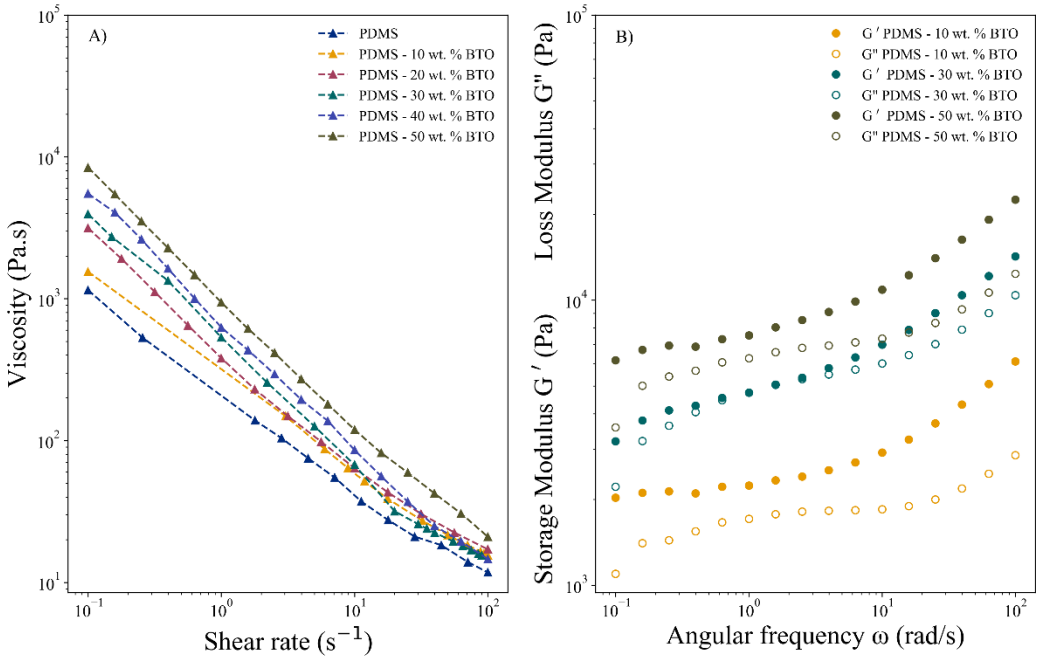

Figure 1. (a) Evolution of viscosity as a function of shear rate at different BTO content (b) Storage and Loss modulus as a function of angular frequency.

For the conductive ink, the MWCNT content plays the most important role to determine the printability and viscosity, since there is a minimal weight percentage required to reach the percolation threshold. The conductivity percolation threshold was reached at 11 wt. % of MWCNT, which represents 34.14 vol. % of

functional filler dispersed on the PDMS matrix. The viscosity measurements on the PDMS-MWCNT ink using both PDMS (Dowsil 1700 and Dow Sygard 184 used in 8:2 ratio respectively) showed a high viscosity (< 2140 Pa.s) at low shear rates due to the high MWCNT content on the ink as shown in Figure 2 (a). This high viscous ink exceeded the capabilities of the extruder head and thus it was considered not suitable for printing, as it might affect the flowability resulting on a non-continuous material deposition (Supplemental Figure S1). For that reason, a PDMS-MWCNT ink using PDMS Dow Sygard 184 as the matrix was developed using 11 wt. % MWCNT, which showed a reasonable decrease in the viscosity compared with using both PDMS in the matrix as shown in Figure 2(a). This PDMS-MWCNT ink was adaptable for 3D printing as it showed a shear thinning behavior and a solid-like behavior as demonstrated in Figure 2 (b) and thus self-support capabilities.

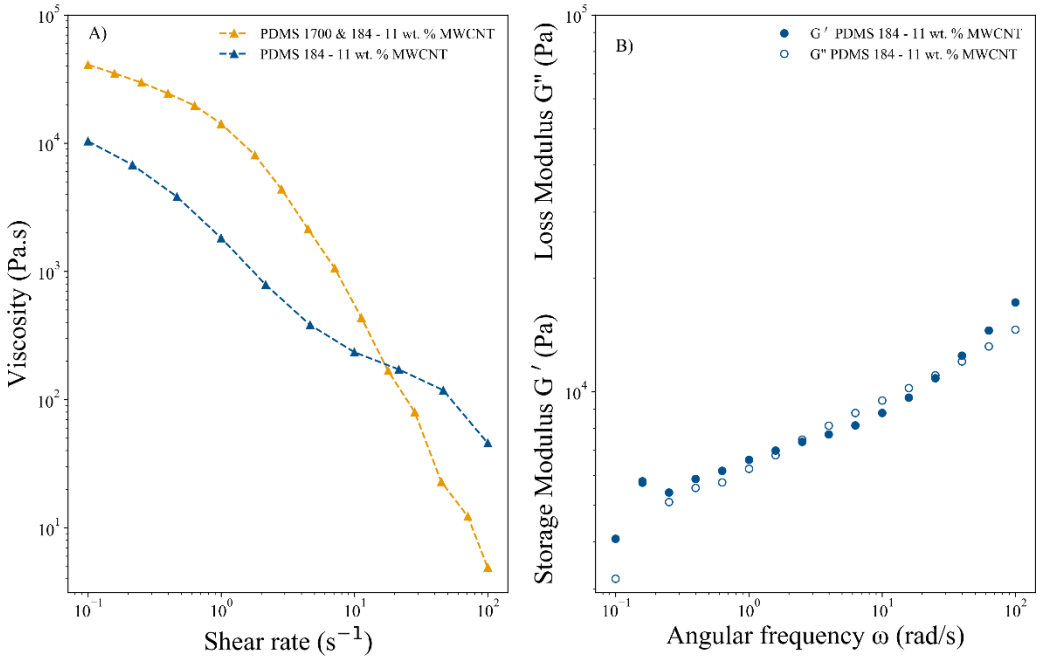

Figure 2. Viscosity of the MWCNT as a function of shear rate

3.2 DIW multi-material 3D printing optimization

For this research work, PDMS-BTO and PDMS-CNT composites were necessary for the development of flexible piezoelectric sensors in one-step fabrication. A dual extrusion head configuration was employed to support both materials, as shown in Figure 3 (a) and a program such as Slic3r that is compatible with multiple head setup configuration. The quality of the samples was affected by different printing parameters, such as printing speed, layer height, infill path, and infill density that had to be modified in the g-code on trial-and-error basis until the quality of the print was optimal. One of the factors that had a high impact on the resolution of the samples was the nozzle diameter to control material deposition while avoiding leaving voids during printing, which could be solved by using a smaller nozzle size and by changing printing path on the g-code (Supplemental Figure S2). In addition, the final resolution depended on the nozzle diameter with respect of the printing speed, material flow ratio and layer thickness that controlled the material's continuous deposition [14]. For multi-material extrusion, both nozzles' sizes must match to minimize quality defects produced by the material flow during printing. Supplemental Figure S3 shows how by using the same nozzle diameter for both materials (PDMS-BTO & PDMS-MWCNT) helped to get a constant

layer thickness in both materials and good material bonding when overlapped. After some flow testing, it was established that both inks could be printable using a 500 µm inner diameter nozzle size to achieve good printing quality in both materials by keeping the same printing parameters such as the printing speed, layer height and infill density for both inks. Figure 3 (b) shows material tool change for the deposition of the conductive ink on top of the piezoelectric ink and the completed sample with flexible capabilities.

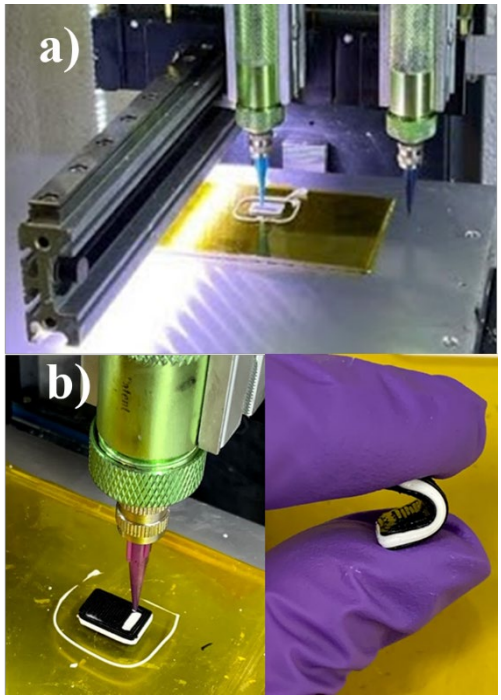

Figure 3. (a) Multi-material printing setup (b) Conductive ink deposition and completed sample after curing.

Multi-material printing technique requires assigning prime/unprime values in the g-code to control material flow and retraction of the material on non-printing moves or while changing the printing head tool. These prime/unprime values results in having precise deposition of each material when it is needed and thus giving it better resolution to the samples. Moreover, a controlled prime/unprime settings eliminate undesired material leakage when triggering a tool change that could affect the quality of the sample [15]. In addition, it was found that prime and unprime values depended directly on the viscosity of each material and were set separately on a trial-and-error basis. Table 1 shows the parameter values for prime (advance) and unprime (retract) of the inks used for multi-material printing. The motor steps controlled the number of pulses to feed the material, which must be assigned considering the viscosity of the ink, the PDMS-BTO ink required higher motor steps for a proper prime/unprime settings due to its lower viscosity range as shown in the rheological results. In contrast, due to the high viscosity of the PDMS-MWCNT ink, it was necessary to reduce motor steps to avoid material overflow during printing. In addition, motor rate controlled the speed of the prime/unprime values, which was left with the default settings as recommended by the manufactured. Lastly, the dwelling time determined the waiting time to execute prime/unprime before moving, where it was determined that the PDMS-BTO ink required a higher dwelling time due to the lower viscosity range.

Table 1. Printing configuration for multi-material deposition

Parameter for Prime / Unprime	PDMS-MWCNT	PDMS-BTO
Motor Steps No.	15000	20000
Motor Rate	15000	15000
Dwelling Time - ms	400	500

During the printing process, it was noticed that after depositing the PDMS-BTO ink on the substrate there was an expansion of the material, which seemed to be influenced by the viscosity of the composite. This was perceived by the naked eye, as a clear overaccumulation of the material was produced while printing the infill path resulting in bad quality samples (Supplementary Figure S4). This anomaly was more evident for the inks with lower BTO content in the PDMS matrix, as the viscosity was decreased. To solve this issue with the expansion of the material, different extrusion rates for the PDMS-BTO printing head were tested aiming to determine an adequate value valid for all the PDMS-BTO inks. First, the extrusion rate was reduced by 40% leading to a 0.6 factor which came to have gaps in the final print. Eventually a 0.85 extrusion rate was assigned to the printing head used for BTO-PDMS which gave the best quality results for this material. The PDMS-MWCNT ink was used with the default material extrusion of 1.0 as the material flow was continuous while printing. Figure 4 illustrates different geometries printed using DIW multi-material technique that can be further used for mechanical testing.

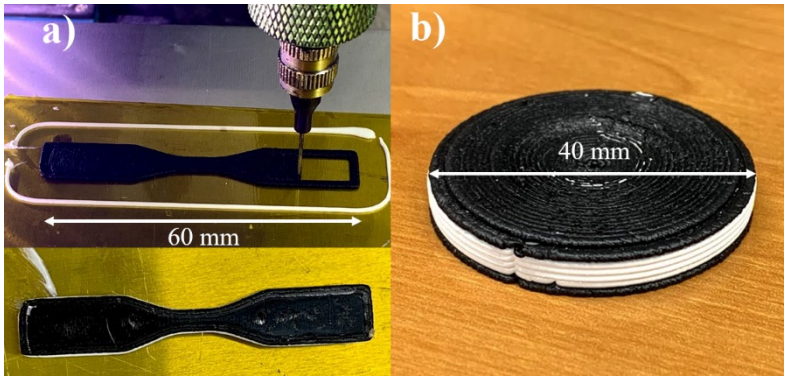

Figure 4. Samples printed by DIW multi-material printing after curing (a) Dogbone for tensile testing (b) Disk for cyclic compression

3.3 Composites microstructure

The samples microstructure was characterized from the cross-section area by SEM to observe the interface between piezoelectric composites and electrodes as shown in Figure 5. There were no indications of delamination between the sensor and electrodes, which indexed for good material bonding as it was fabricated and cured in one-step. The sample had only few voids or air bubbles, which might have been produced either during printing or curing process. Figure 6 shows the BTO particles dispersed on the thermoset matrix, the samples did not show evident agglomerations of powders, which could indicate that the planetary mixer was beneficial to the ink fabrication. In addition, a good filler dispersion could be favorable to obtain a uniform piezoelectric response after polarization [maybe add Hoejin's paper here]. (https://journals.sagepub.com/doi/full/10.1177/0021998317704709)

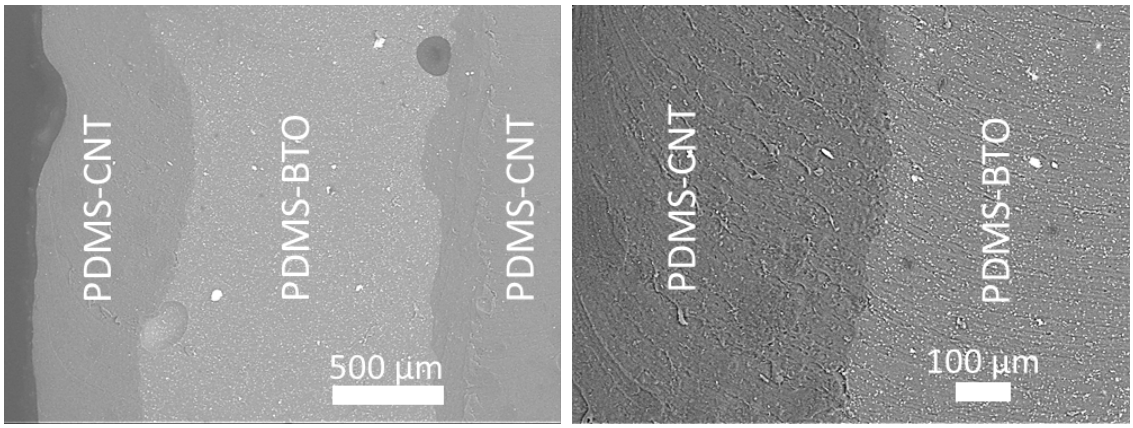

Figure 5. PDMS-BTO and PDMS-MWCNT bonding

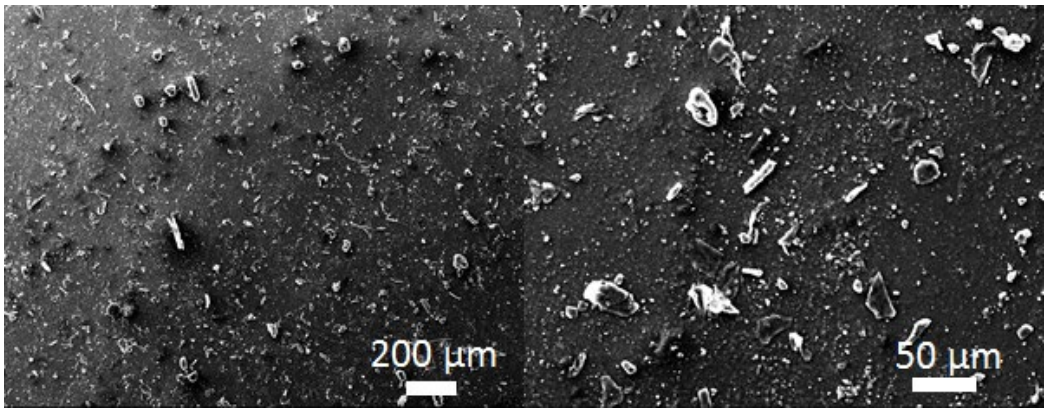

Figure 6. BTO dispersion on the PDMS matrix

3.4 Piezoelectric and dielectric properties

The samples were polarized by corona poling, which is a non-contact method that discharges ionized air between sharp needles and a ground electrode as a result of a high applied voltage [5], [6], [16]. Corona poling is typically used in the polarization of piezoelectric polymer composites since it allows to apply high voltage without producing an electrical shortage. Figure 5 (a) illustrates the electrical circuit for the multi-needle corona poling setup used for the polarization of the PDMS-BTO composites. The high-power voltage supply was connected to five copper needles that were attached together with copper tape while the copper block worked as the bottom electrode, which was connected to ground to avoid electrical shortage and placed on top of a hot plate. As illustrated in Figure 7 (b) a purple beam also referred as ionized air impacted the surface of the sample, which allowed the alignment of the BTO's dipoles in the PDMS matrix that gave it piezoelectric properties.

Several factors affected the effectivity of the PDMS-BTO polarization through corona poling discharge, including applied voltage, distance from needle to electrode, temperature and time of polarization [16]. Table 2 summaries the parameters evaluated for poling of the piezoelectric composites. It was found that a minimal applied electrical field of 5.5 kV/cm was required to polarize the samples, where a more effective polarization process was observed by increasing the electrical field up to 8 kV/cm. On the other hand, the distance between needle and electrode played an important role as it was required that the corona beam impacted completely the whole surface of the sample. In addition, it was noticed that using a distance below 2 cm for the bigger samples (Ø < 40 mm) resulted on uneven polarization, as non-uniform d_{33} values were

obtained and where the highest d_{33} value was observed only where the corona beam impacted directly during poling. Applying temperature during poling helps to facilitate the dipoles alignment, for that reason, temperature was evaluated below BTO's curie temperature (T_c = 120 °C) in a range from room temperature (RT) to 80 °C. Although it was possible to polarize the composites at RT, a better piezoelectric response was observed at higher temperatures. Lastly, the poling time was evaluated from 1.5 to 2 hours, which had close to none influence on the poling process. After some experimentation, it was established that the optimal results to polarize the PDMS-BTO samples was applying an electrical field of 8 kV/cm with a distance from needle to electrode of 3 cm at 80 °C for two hours.

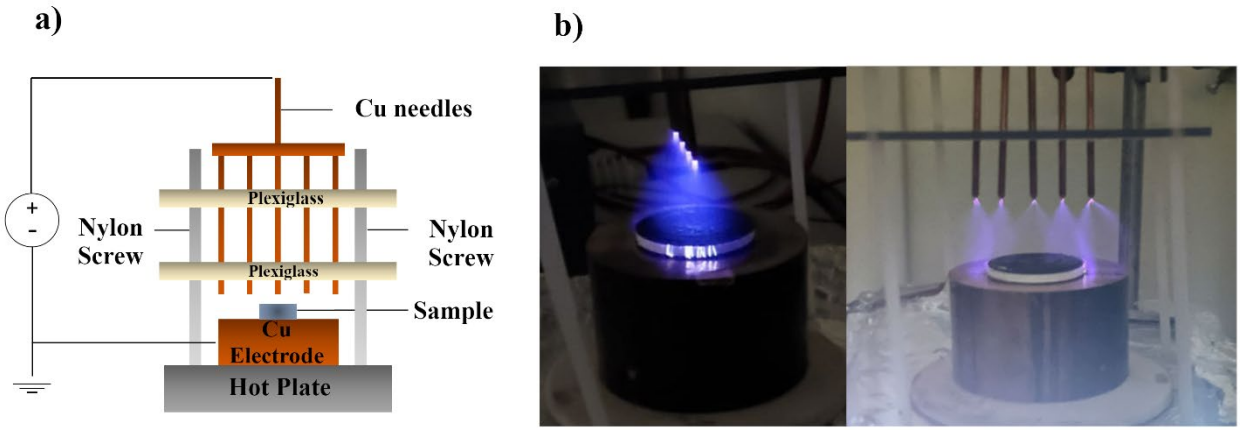

Figure 7. (a) Electric circuit for multi-needle corona poling. (b) Sample under corona beam impact

Table 2. Parameters for corona poling discharge optimization

Electrical field	Distance	Temperature	Time	Poling
5.5 kV/cm	1.5 cm	70 °C	1.5 hours	Yes
4.1 kV/cm	2 cm	RT	2 hours	No
4.1 kV/cm	2 cm	80 °C	2 hours	No
6 kV/cm	2 cm	70 °C	1.5 hours	Yes
8 kV/cm	3 cm	RT	2 hours	Yes
8 kV/cm	3 cm	80 °C	2 hours	Yes

The piezoelectric coupling coefficient (d_{33}) was evaluated to determine the effectivity of the polarization of BTO particles dispersed in the PDMS matrix. Figure 8 (a) shows the piezoelectric coefficient d_{33} of the 3D printed samples at different content of BTO particles expressed as weight percent. It was shown that the piezoelectric response was directly influenced by the BTO wt. % content, in which higher fillers led to higher d_{33}. The highest piezoelectric coupling coefficient was observed on 50 wt. % BTO (~ 13.8 vol. % BTO) samples with a d_{33} of 11.5 pC/N which represent a 6.02 % of theoretical properties. It demonstrates the efficiency of the poling method. These results are in good agreement with literature as polarization of 10 vol. % of PZT dispersed on a silicone matrix showed a d_{33} of 10.22 % theoretical properties [17]. The results obtained in piezoelectricity could be explained with the particle size of BTO (Supplemental Figure S5) used in the fabrication of the composites. It was noticed that the BTO's particle size was close to 1 micron, which has been found to be beneficial to the crystalline structure of BTO and contribute to a higher piezoelectric response [18], [19]. However, the BTO particles had high variation on their size affecting the piezoelectric response after polarization. In addition, since the BTO particles are not subjected to a heat

treatment process such as sintering, there is no further grain grow of BTO particles and thus limiting the piezoelectricity [20]. The relative dielectric permittivity of the samples (Figure S6) was measured at 1 kHz. It was observed that there was no significant difference in dielectric permittivity measured for PDMS-BTO composites, where the highest results were observed for the 50 wt. % BTO with dielectric permittivity of 10. The low relative dielectric permittivity could be attributed to the PDMS matrix that acts an electrical insulator and thus decreasing dielectric permittivity [21]. The influence of the BTO filler in the thermoset matrix with respect the stretchability (elongation at break) was determined by testing three samples under tension according to the ASTM D412 for elastomers. Figure 8 (b) presents the elongation at break % for PDMS-BTO composites and PDMS, which was tested as control. It was observed how the elongation at break decreases with respect the increment of BTO content in the PDMS matrix, which was an expected behavior for samples with higher content of BTO. However, the elongation at break for the composites with 50 wt. % BTO still showed a high degree of flexibility and compliance with a maximum elongation at break observed at 76.5 %, which represents 63.75 % of the elongation at break obtained for PDMS samples.

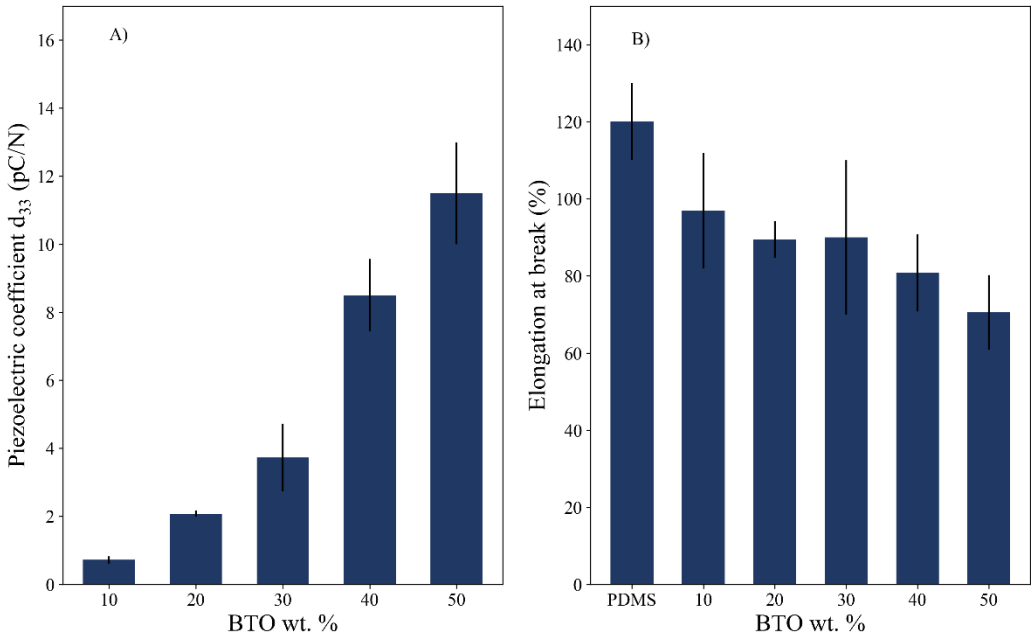

Figure 8. PDMS-BTO composites at different filler contents (a) Piezoelectric properties (b) Elongation at break

To demonstrate the force sensing capability, the output voltage from printed PDMS-BTO composites were measures with an oscilloscope and a fatigue load frame under a cyclic compression loading as shown in the schematic representation in Figure S7. The load frame was set under a maximum compression load of around 200 lbF for 10 cycles and using a speed of 500 mm/min as illustrated in Figure 9, while the oscilloscope measured the produced voltage as a result of the applied load. Figure 10 shows the voltage output measured from PDMS-BTO composites at different filler content after polarization. It was noticed an increment on the produced voltage when increasing the piezoelectric filler in the PDMS matrix due to higher d_{33}. The samples were exposed to a mechanical stress under compression that resulted in a positive voltage response from the piezoelectric sample while when releasing such stress produced a negative voltage. The shape of the periodic output voltage obtained for the PDMS-BTO composites were consistent

with other reported piezoelectric sensors [22], [23]. A positive output voltage was observed at 37 mV, 60 mV, 78 mV, 135 mV, and 250 mV while a negative voltage of -18 mV, -60 mV, -46 mV, -108 mV, and -135 mV for the 10 wt. %, 20 wt. %, 30 wt. %, 40 wt. % and 50 wt. % BTO respectively. It was observed that the voltage output measured from peak-to-peak linearly increased with respect the BTO content in the composite and the response time to an applied mechanical stress was faster for samples more with BTO content. The highest voltage output of 385 mV was measured from peak-to-peak for the 50 wt. % BTO-PDMS composites. These results demonstrate the capability of using DIW multi-material technique in the fabrication of functional sensors with high stretchability in one-step fabrication.

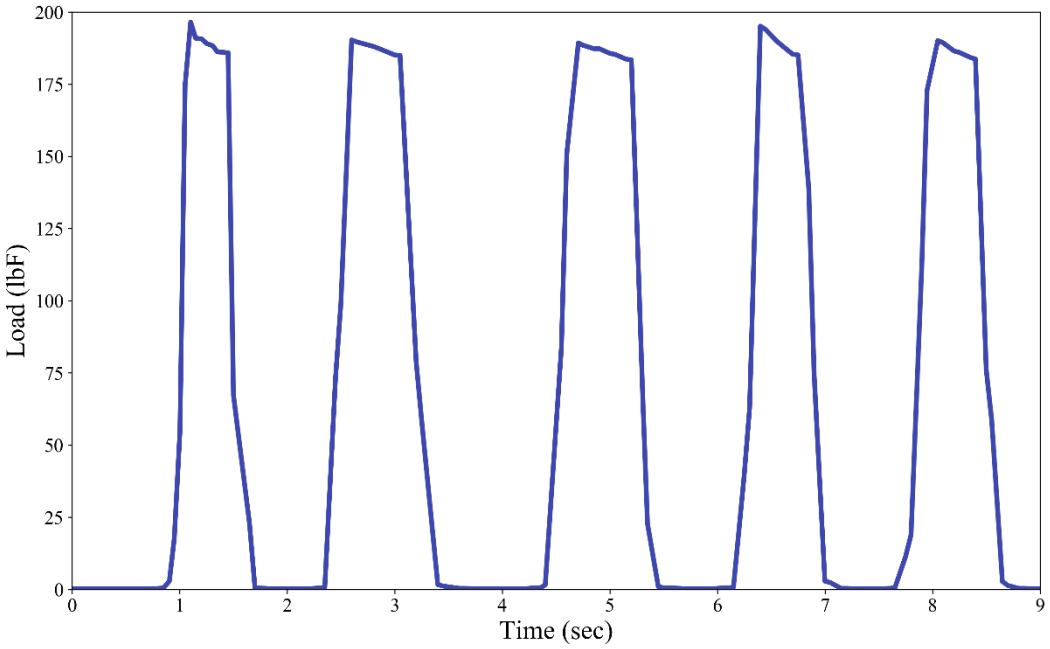

Figure 9. Cyclic load applied on samples under compression.

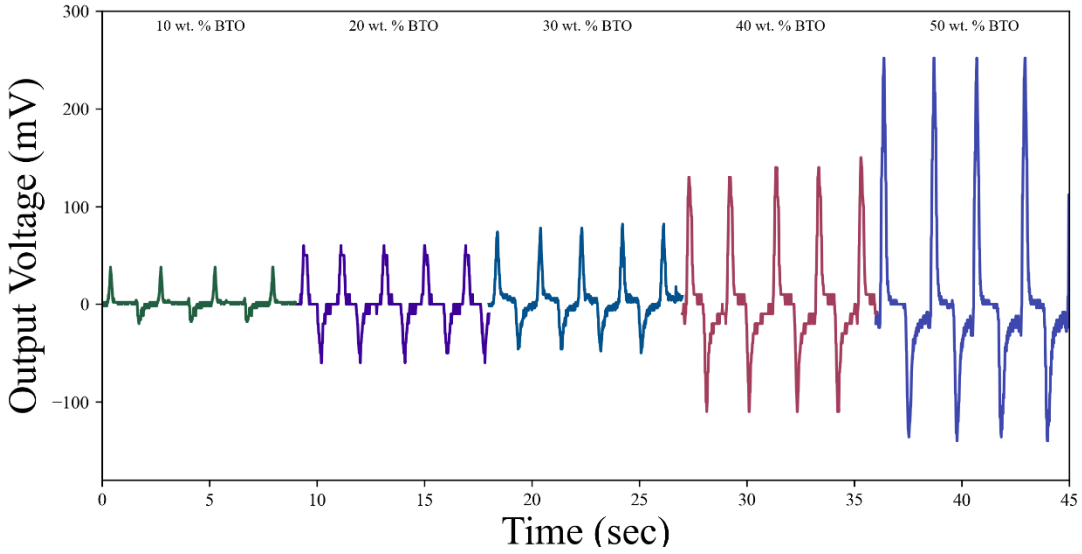

Figure 10. Output voltage of PDMS-BTO composites at different filler contents.

4. Conclusion

Due to the advancements in AM technology, multi-material DIW printing was made possible through the advancement in technology which allowed it to be more beneficial in newer forms of fabrication compared to traditional fabrication methods, such as casting in order to fabricate and print an elastic composite for one-step sensors applications. In this work, it was shown a novel approach in the fabrication of PDMS-BTO composites to create a compromising flexible device through multi-material DIW printing with high piezoelectric coefficients. The percolation threshold was reached by using 11 wt. % MWCNT dispersed on the PDMS matrix, which worked as an electrode that allowed the BTO's dipoles alignment making it applicable for force sensors applications. Through the capabilities of DIW printing of multi-material, it has allowed optimization by defining printing parameters such as nozzle size, layer height, etc., which was applicable for both inks and allowed an improvement in the material bonding between PDMS-BTO and electrodes (PDMS-MWCNT). The PDMS-BTO sensors, evaluated from 10-50 wt. % BTO were subjected to corona poling to align the BTO dipoles. It was found that the piezoelectric properties depended on the BTO content in the composite indicating higher piezoelectric properties with higher BTO content. By fabricating 50 wt. % BTO with PDMS the material showed the highest piezoelectric coefficient (d_{33}) of 11.5 pC/N that gave the highest output voltage of 385 mV under constant compression loading of >200 lbF. All printed samples showed great elastic properties due to PDMS stretchable properties which makes it ideal for further applications in biomedical fields. A current drawback to including higher content of BTO particles ultimately lowers the elastic properties creating a threshold between piezoelectric and elastic properties. However, the samples maintained good elasticity to compliance to different surfaces and capture pressure signals. This has allowed the fabrication of high stretchable force sensors with one-step fabrication process that gave relatively high piezoelectric coefficient properties which will inspire future work in various selection of multi-materials of DIW printing.

References

[1] T. R. Shrout and S. Zhang, "Lead-free piezoelectric ceramics: Alternatives for PZT?," *Journal of Electroceramics*, vol. 19, no. 1, Sep. 2007, doi: 10.1007/s10832-007-9095-5.

[2] G. H. Haertling, “Ferroelectric Ceramics: History and Technology,” *Journal of the American Ceramic Society*, vol. 82, no. 4, pp. 797–818, 1999, doi: 10.1111/j.1151-2916.1999.tb01840.x.
[3] M. Cheng *et al.*, “A review of flexible force sensors for human health monitoring,” *Journal of Advanced Research*, vol. 26, pp. 53–68, Nov. 2020, doi: 10.1016/j.jare.2020.07.001.
[4] M. P. Wolf, G. B. Salieb-Beugelaar, and P. Hunziker, “PDMS with designer functionalities—Properties, modifications strategies, and applications,” *Progress in Polymer Science*, vol. 83, pp. 97–134, Aug. 2018, doi: 10.1016/j.progpolymsci.2018.06.001.
[5] K. k Sappati and S. Bhadra, “0-3 Barium Titanate-PDMS Flexible Film for Tactile Sensing,” in *2020 IEEE International Instrumentation and Measurement Technology Conference (I2MTC)*, May 2020, pp. 1–6. doi: 10.1109/I2MTC43012.2020.9128512.
[6] K. K. Sappati and S. Bhadra, “Flexible Piezoelectric 0–3 PZT-PDMS Thin Film for Tactile Sensing,” *IEEE Sensors Journal*, vol. 20, no. 9, pp. 4610–4617, May 2020, doi: 10.1109/JSEN.2020.2965083.
[7] A. Nag, S. Feng, S. C. Mukhopadhyay, J. Kosel, and D. Inglis, “3D printed mould-based graphite/PDMS sensor for low-force applications,” *Sensors and Actuators A: Physical*, vol. 280, pp. 525–534, Sep. 2018, doi: 10.1016/j.sna.2018.08.028.
[8] J. A. Lewis, “Direct Ink Writing of 3D Functional Materials,” *Advanced Functional Materials*, vol. 16, no. 17, pp. 2193–2204, 2006, doi: 10.1002/adfm.200600434.
[9] A. Renteria *et al.*, “Particle size influence on material properties of BaTiO3 ceramics fabricated using freeze-form extrusion 3D printing,” *Mater. Res. Express*, vol. 6, no. 11, p. 115211, Oct. 2019, doi: 10.1088/2053-1591/ab4a36.
[10] W. Li, A. Ghazanfari, D. McMillen, M. C. Leu, G. E. Hilmas, and J. Watts, “Fabricating ceramic components with water dissolvable support structures by the Ceramic On-Demand Extrusion process,” *CIRP Annals*, vol. 66, no. 1, pp. 225–228, Jan. 2017, doi: 10.1016/j.cirp.2017.04.129.
[11] Y. Guo, Y. Liu, J. Liu, J. Zhao, H. Zhang, and Z. Zhang, “Shape memory epoxy composites with high mechanical performance manufactured by multi-material direct ink writing,” *Composites Part A: Applied Science and Manufacturing*, vol. 135, p. 105903, Aug. 2020, doi: 10.1016/j.compositesa.2020.105903.
[12] T. Kaully, A. Siegmann, and D. Shacham, “Rheology of highly filled natural CaCO3 composites. II. Effects of solid loading and particle size distribution on rotational rheometry,” *Polymer Composites*, vol. 28, no. 4, pp. 524–533, 2007, doi: 10.1002/pc.20309.
[13] G. Shi *et al.*, “A versatile PDMS submicrobead/graphene oxide nanocomposite ink for the direct ink writing of wearable micron-scale tactile sensors,” *Applied Materials Today*, vol. 16, pp. 482–492, Sep. 2019, doi: 10.1016/j.apmt.2019.06.016.
[14] H. Yuk and X. Zhao, “A New 3D Printing Strategy by Harnessing Deformation, Instability, and Fracture of Viscoelastic Inks,” *Advanced Materials*, vol. 30, no. 6, p. 1704028, 2018, doi: 10.1002/adma.201704028.
[15] H. Nassar, M. Ntagios, W. T. Navaraj, and R. Dahiva, “Multi-Material 3D Printed Bendable Smart Sensing Structures,” in *2018 IEEE SENSORS*, Oct. 2018, pp. 1–4. doi: 10.1109/ICSENS.2018.8589625.
[16] M. Rotan, M. Zhuk, and J. Glaum, “Activation of ferroelectric implant ceramics by corona discharge poling,” *Journal of the European Ceramic Society*, vol. 40, no. 15, pp. 5402–5409, Dec. 2020, doi: 10.1016/j.jeurceramsoc.2020.06.058.
[17] S. Mamada, N. Yaguchi, M. Hansaka, M. Yamato, and H. Yoshida, “Matrix influence on the piezoelectric properties of piezoelectric ceramic/polymer composite exhibiting particle alignment,” *Journal of Applied Polymer Science*, vol. 132, no. 15, 2015, doi: 10.1002/app.41817.
[18] V. Buscaglia and C. A. Randall, “Size and scaling effects in barium titanate. An overview,” *Journal of the European Ceramic Society*, vol. 40, no. 11, pp. 3744–3758, Sep. 2020, doi: 10.1016/j.jeurceramsoc.2020.01.021.
[19] A. Renteria *et al.*, “Influence of bimodal particle distribution on material properties of BaTiO3 fabricated by paste extrusion 3D printing,” *Ceramics International*, vol. 47, no. 13, pp. 18477–18486, Jul. 2021, doi: 10.1016/j.ceramint.2021.03.171.

[20] J. L. Zhang, P. F. Ji, Y. Q. Wu, X. Zhao, Y. Q. Tan, and C. L. Wang, "Strong piezoelectricity exhibited by large-grained BaTiO3 ceramics," *Appl. Phys. Lett.*, vol. 104, no. 22, p. 222909, Jun. 2014, doi: 10.1063/1.4881597.
[21] X. Zhang, M.-Q. Le, O. Zahhaf, J.-F. Capsal, P.-J. Cottinet, and L. Petit, "Enhancing dielectric and piezoelectric properties of micro-ZnO/PDMS composite-based dielectrophoresis," *Materials & Design*, vol. 192, p. 108783, Jul. 2020, doi: 10.1016/j.matdes.2020.108783.
[22] Y. Su, C. Dagdeviren, and R. Li, "Measured Output Voltages of Piezoelectric Devices Depend on the Resistance of Voltmeter," *Advanced Functional Materials*, vol. 25, no. 33, pp. 5320–5325, 2015, doi: 10.1002/adfm.201502280.
[23] J. Zhou *et al.*, "Mechanical−Electrical Triggers and Sensors Using Piezoelectric Micowires/Nanowires," *Nano Lett.*, vol. 8, no. 9, pp. 2725–2730, Sep. 2008, doi: 10.1021/nl8010484.